Accounting for the Shapes and Size Distributions of Miniature Endplate Currents

William Van der Kloot* and Ligia A. Naves‡
*Department of Physiology and Biophysics, Health Sciences Center, State University at Stony Brook, Stony Brook, New York 11794-8661 USA, and ‡Department of Biochemistry and Immunology, Federal University of Minas Gerais, Belo Horizonte, Brazil

ABSTRACT The current model does not account adequately for the characteristics of miniature endplate currents (MEPCs). We do not understand their relatively slow rise, the shape of their rise, their variable and sometimes prolonged decay, and the correlation between amplitude and decay time. If we assume that ACh is released from the vesicle through a pore and that the vesicle enlarges as it takes on additional transmitter, the predictions are more like MEPCs. However, previous measurements showed that after quantal size was increased the vesicles in the terminal were not enlarged. This need not be a problem, because some of the ACh is added to vesicles positioned at the active zones, a process known as second-stage loading. By using the false transmitter precursor monoethylcholine we provide additional evidence for second-stage loading. The distribution of quantal sizes at the junction usually does not follow a normal probability distribution; it is skewed to the right. The skew can be accounted for by a model incorporating second-stage loading in which the vesicles are released randomly, without regard to their ACh content. If the vesicles increase in size when they contain more transmitter, only vesicles at the active zone need swell.

INTRODUCTION

Because quanta are the units that underlie synaptic transmission, it is scarcely surprising that currently there is much interest in neurotransmitter quanta in the central nervous system (reviewed by Edwards, 1995). Quanta were first discovered at the frog neuromuscular junction, where the miniature endplate currents (MEPCs) they produce can be measured with the two-electrode voltage clamp or by an extracellular electrode (Katz, 1969). The MEPCs are almost invariably cited as the models to which other synaptic responses are compared.

The classic picture of MEPC generation has been quantitatively modeled by a number of investigators (Wathey et al., 1979; Rosenberry, 1979; Madsen et al., 1984; Salpeter, 1987; Nigmatullin et al., 1988; Parnas et al., 1989; Bartol et al., 1991). They assume that the ACh is released instantaneously from the nerve terminal, presumably as the synaptic vesicle abruptly dumps its contents by exocytosis. Then they calculate the diffusion of the ACh in the cleft, its interaction with the endplate receptor (AChR), followed by the opening of the channels in the receptor, the hydrolysis of the ACh by acetylcholinesterase (AChE), and the closing of the channels. These models are feasible because there are good measurements of the density of AChR and AChE in the synaptic cleft, and of the kinetics of their reactions with ACh (Salpeter, 1987). The usual MEPC is due to the opening of 1000–2000 ion channels in the AChR in the endplate membrane. Two thousand AChRs lie within a 0.23-μm radius from the point of release. The ACh can diffuse to these 2000 receptors in less than 50 μs. The models suggest the ACh concentration in the cleft drops rapidly, as transmitter is bound to AChR and destroyed by AChE. By the time the peak number of endplate channels has opened, the ACh concentration falls to such a low level that few more channels are opened. Consequently, the decay of the MEPC is determined by the random closings of the receptor channels, which have a mean open time of about 1000 μs.

This classical model accounts reasonably well for most of the features of MEPCs in untreated preparations—hence it has been widely accepted for more than 20 years (Magleby and Stevens, 1972; Edmonds et al., 1995). We first became concerned about the model when we studied the large MEPCs observed after treatments that increase quantal size (Van der Kloot and Van der Kloot, 1986; Van der Kloot, 1987, 1991b). Many of the large MEPCs clearly have longer rise times and slower decays than predicted by the model. Gradually we came to realize that MEPCs from untreated preparations may share the same discrepancies. We will document these discrepancies with results from the literature and with new experiments. Then we will suggest how the classical model can be modified to account for the observations.

Another question about MEPCs is the distribution of their sizes. They usually do not follow a normal probability distribution function; instead their distribution is skewed to the right (Van der Kloot, 1987, 1989, 1991a,b). The skewing is particularly noticeable after quantal size has been enlarged. We will also present a hypothesis to account for the skewing of MEPC sizes and suggest how this model can be tested.

Received for publication 3 November 1995 and in final form 7 February 1996.

Address reprint requests to Dr. William G. Van der Kloot, Department of Physiology and Biophysics, SUNY at Stony Brook, Health Sciences Center, Stony Brook, NY 11794-8661. Tel.: 516-444-3035; Fax: 516-444-3432; E-mail: wvanderkloot@sbccmail.bitnet.

0006-3495/96/05/2175/10 $2.00

MATERIALS AND METHODS

Data recording

MEPCs were recorded from junctions in the frog, *Rana pipiens*, in sartorius or cutaneous pectoris muscles. The preparations were in a Ringer's that contained (in mM): NaCl, 120; KCl, 2.0; $CaCl_2$, 2.5; and *N*-tris-(hydroxymethyl) methyl-2-aminoethanesulfonic acid/NaOH (TES), 4.0 at pH 7.4. In hypertonic gluconate solution the NaCl was replaced with 200 mM Na gluconate.

The methods for preparing the electrodes, performing the two-electrode voltage clamp, and capturing the data on a computer are given by Van der Kloot et al. (1994). The methods for recording the extracellular miniature endplate potentials (MEPPs) are given by Van der Kloot (1995). However, we no longer use a digital delay. Instead, the recordings were obtained using a DAS16/330 A/D converter from ComputerBoards (Mansfield, MA), which can be programmed to store a predetermined number of samples before and after a trigger pulse. This eliminates the need for a digital delay. The software sampling routines were also from ComputerBoards. The programming was done in Turbo Pascal. There is a problem with the system when the board is programmed to take in a series of sweeps: on occasion it freezes. By chance we found that the program will resume if the operator keys in a "break" followed by a "control-break." The differentiation was done by a numerical method (Stavitzy and Golay, 1964).

Modeling

We used the model of MEPC generation developed by Wathey et al. (1979). In this model the ACh simply diffuses in circular coordinates from the point of release. There are more geometrically accurate models (Madsen et al., 1984; Nigmatullin et al., 1988; Parnas et al., 1989). The most comprehensive model uses Monte Carlo methods to follow individual ACh molecules diffusing in three dimensions in a much more realistic geometry (Salpeter, 1987; Bartol et al., 1991). But there seems to be little difference in the predictions of the simple and the more complex models. The values for the parameters come from Wathey et al. (1979); they are given in parentheses when the parameters are defined. In the model a quantum of ACh (10,000 molecules) is released from the terminal at a point facing the center of a circular endplate. The ACh is distributed over a circle with the radius of a synaptic vesicle (0.025 μm), with the highest concentration in the center of this circle and with the concentration declining toward the edge (in an approximation to a gaussian). The [ACh] in the cleft is abbreviated as a. The radial coordinate r (0.5 μm) is the distance from the center of the cleft to its edge. At the edge the cleft is open to the external solution. Diffusion of a from the points of release is given by

$$\left.\frac{\delta a}{\delta t}\right]_{\text{diffusion}} = D\left(\frac{\delta^2 a}{\delta r^2} + \frac{1}{r}\frac{\delta a}{\delta r}\right), \tag{1}$$

where D is the diffusion coefficient for ACh (3×10^{-6} cm^2 s^{-1}). If AChE is present the rate of ACh hydrolysis is given by

$$\left.\frac{\delta a}{\delta t}\right]_{\text{hydrolysis}} = -k_1(e_o - e^A)a, \tag{2}$$

where k_1 is the binding constant (2×10^8 M^{-1} s^{-1}), e_o (2,600 sites/(μm^2)) is the concentration of AChE, and e^A is the concentration of AChE that has bound an ACh:

$$\frac{\delta e^A}{\delta t} = k_1(e_o - e^A) - k_3 e^A, \tag{3}$$

where k_3 is the turnover rate (1.6×10^4 s^{-1}). The binding of ACh to AChR is given by

$$\left.\frac{\delta a}{\delta t}\right]_{\text{receptors}} = -2k_{+1}(c_0 - c^1 - c^{11})a - k_{+2}c^1 a + k_{-1}c^1 + 2k_{-2}c^{11}, \tag{4}$$

where k_{+1} is the binding rate of ACh to the unoccupied receptor (1.5×10^8 M^{-1} s^{-1}), k_{-1} is the disassociation rate of ACh from the singly occupied receptor (7.5×10^3 s^{-1}), k_{+2} is the binding rate of ACh to the singly occupied receptor (3×10^7 M^{-1} s^{-1}), k_{-2} is the dissociation rate of ACh from the doubly occupied receptor, c_0 is the concentration of AChR (12,000/μm^2), c^1 is the concentration of singly occupied receptor, and c^{11} is the concentration of doubly occupied receptor

$$\frac{\delta c^1}{\delta t} = 2k_{+1}(c_0 - c^1 - c^{11})a + 2k_{-2}c^{11} - K_{+2}c^1 a - k_{-1}c^1 \tag{5}$$

$$\frac{\delta c^{11}}{\delta t} = k_{+2}c^1 a - 2k_{-2}c^{11}. \tag{6}$$

We also calculated the rate of channel opening, δchan/δt:

$$\frac{\delta \text{chan}}{\delta t} = k_{+2}c^{11}a. \tag{7}$$

The equations for diffusion were replaced with finite difference approximations for radial coordinates. The simultaneous equations were solved by the Runge-Kutta-Fehlberg method, which estimates the truncation error at each step, so that the time step could be adjusted to keep within a predetermined error. Calculations began with a temporary synaptic radius of twice the vesicle diameter, so that δr was small, and then as the ACh diffused outward, δr was increased stepwise until it reached the full radius of the cleft.

We calculated the effects of release through a pore by combining Eq. 8 (given in the Results) with the Wathey et al. (1979) model (Van der Kloot, 1995). The pore length was 1×10^{-6} cm, and the diffusion coefficient for ACh in the vesicle and pore was 4×10^{-6} cm^2 s^{-1}. When the quantum contained 10,000 ACh molecules the vesicle volume was 2.65×10^{-17} cm^3. In a variation of this model, as the ACh content was varied, the vesicle volume was changed to keep the ACh concentration in the vesicle constant. The pore radius was 0.08×10^{-6} cm.

We modeled the open time of an endplate AChR by $-\ln(rd)$, where rd is a random number between 0 and 1. This step was repeated 1000 times, and the resulting array of open times was sorted in ascending order. The open time of the 500th event was taken as the $t_{1/2}$ of the model MEPC. This sequence was repeated 100 times, to give the range of values expected in one data set. We continued the process until we had accumulated 100 model data sets.

We modeled the effects by second-stage loading on the size distribution of MEPCs as follows. The vesicles first acquired ACh in the cytoplasm by a gaussian process that gave them a mean content with a CV of 10%. They then were attached to the active zones. With each time step a randomly selected fraction of those on active zones were released, those remaining on the active zone each received a gaussian addition of ACh (CV = 10%). The empty positions on the active zone acquired vesicles from the cytoplasm. The rate of ACh addition at the active zones was varied so that the mean amount added reached the desired level. This was done empirically, by selecting a rate of second-stage loading, running the model until the size of the quanta released arrived at an asymptote, and then modifying the rate until the model produced the required mean quantal size.

RESULTS

The shape of the rise of the miniatures

The rise times of frog MEPCs and of MEPPs recorded with an extracellular electrode appear to be slower than predicted by the classical model (Dwyer, 1981; Van der Kloot, 1995). The rate of rise of the MEPC might be slower than predicted because the ACh is released from the vesicle through a narrow pore, or because it takes time for the cationic ACh

to dissociate from anions in the vesicle wall or interior (Nanavati and Fernandez, 1993). There is substantial evidence that release from mast cells and adrenal chromaffin cells is through a pore (Spruce et al., 1990; Monck and Fernandez, 1992; Chow et al., 1992).

Further evidence comes from an examination of the shape of the rise of the endplate current and its differential, because predictions of the classical model and the pore model are quite different. The classical model predicts that channels will open most rapidly at the beginning, and that the rate of opening will fall off progressively as the MEPC rises (Fig. 1 *A*). The pore model predicts that the rise will be sigmoid, with the rate of channel opening rising and then decreasing during the upstroke of the MEPC (Fig. 1 *B*). Recordings of rise times with extracellular electrodes show that their shapes resemble the predictions of the pore model and are quite different from the predictions of the classic model (Fig. 1 *C*). The record shown is typical of the 47 externals from five junctions that were examined.

The variance of the decay times

Previous work with preparations in which quantal size was experimentally enlarged showed that decay times are often much longer than predicted by the closing times of the endplate channels (Van der Kloot, 1991b). The present experiments suggest that for many MEPCs in untreated preparations the decay times also do not fit the predictions. An example of the output of the classical model of Wathey et al. (1979) is shown in Fig. 2 *A*, along with a real MEPC from an untreated preparation. To make comparisons by eye easier, the model MEPC was normalized so that its peak inward current was the same as the real MEPC. Obviously the model in the figure decays much faster than the MEPC. The discrepancy occurs because we selected one of the longest MEPCs from a set of 121 recorded at the same junction. Fig. 2 *B* illustrates some of the variation seen in the MEPCs in this set. If we had chosen one of the shorter MEPCs in the set, its decay would be fit well by the model. Fig. 2 *C* shows the variation in decay times seen in a typical data set. The points are plotted on a probability scale, which is used because the points fall along a straight line if they follow a normal probability distribution function (Sokal and Rohlf, 1981; Van der Kloot, 1989). The variance of the data is proportional to the slope of the line. The decay times in Fig. 2 *C* do not fall along a line, but on an ascending curve, which means that when plotted as a histogram the bins would be skewed to the right. This skewing is also typical of plots of MEPC amplitudes or areas (Van der Kloot and Van der Kloot, 1986; Van der Kloot, 1989, 1991b). We will return to the problem of the skewing later.

We would expect some variation in the decay times within a set because the ACh opens a large number of channels with random, exponentially distributed lifetimes. Such random variations lead to scatter in the decay times of the MEPCs, which can be easily modeled, as is also shown in Fig. 2 *C*. With 1000 channels opening, the coefficient of variation (CV) of modeled half decay times was 0.04 ± 0.0054 (SD). We did not include in this calculation the additional variance expected from the jitter in the rise times, because Monte Carlo modeling suggests that it is negligible (see figure 4 in Anglister et al., 1994). The variation is much less than predicted for central synapses, where fewer transmitter molecules are in each quantum (Faber et al., 1992). The variance in the decay times from real MEPCs is higher than predicted by the model. From 133 sets of measurements with the two-electrode voltage clamp on the frog cutaneous pectoris muscle (each set containing about 100 MEPCs), the mean CV was 0.17 ± 0.032, more than four times higher than the model predicts. The probability that the differences between the CVs of the model and the data is by chance is $<10^{-6}$. From six sets of measurements with extracellular electrodes, which have less instrumental noise, the mean CV was 0.14 ± 0.035. The classical model does not account for the observed scatter of the decay times. At the frog neuromuscular junction there is no evidence for different receptor types, with different mean open times

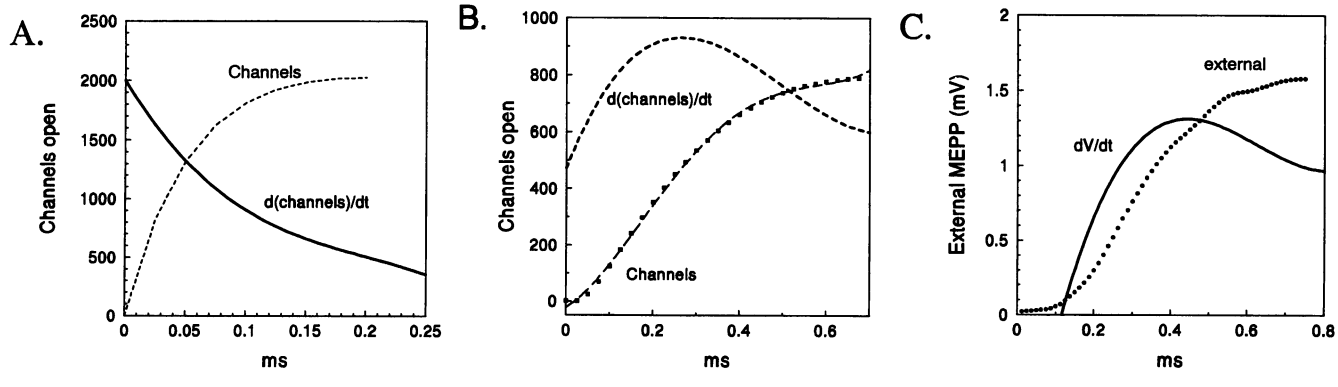

FIGURE 1 Predictions and measurements of the rise and rate of rise of miniatures. (*A*) The prediction of the classic model (– – –) and its differential (——). (*B*) The prediction of a model in which release is through a pore (·····) and its differential (– – –). (*C*) A typical measurement of the rise of an externally recorded miniature at 10°C (·····) and its differential (——).

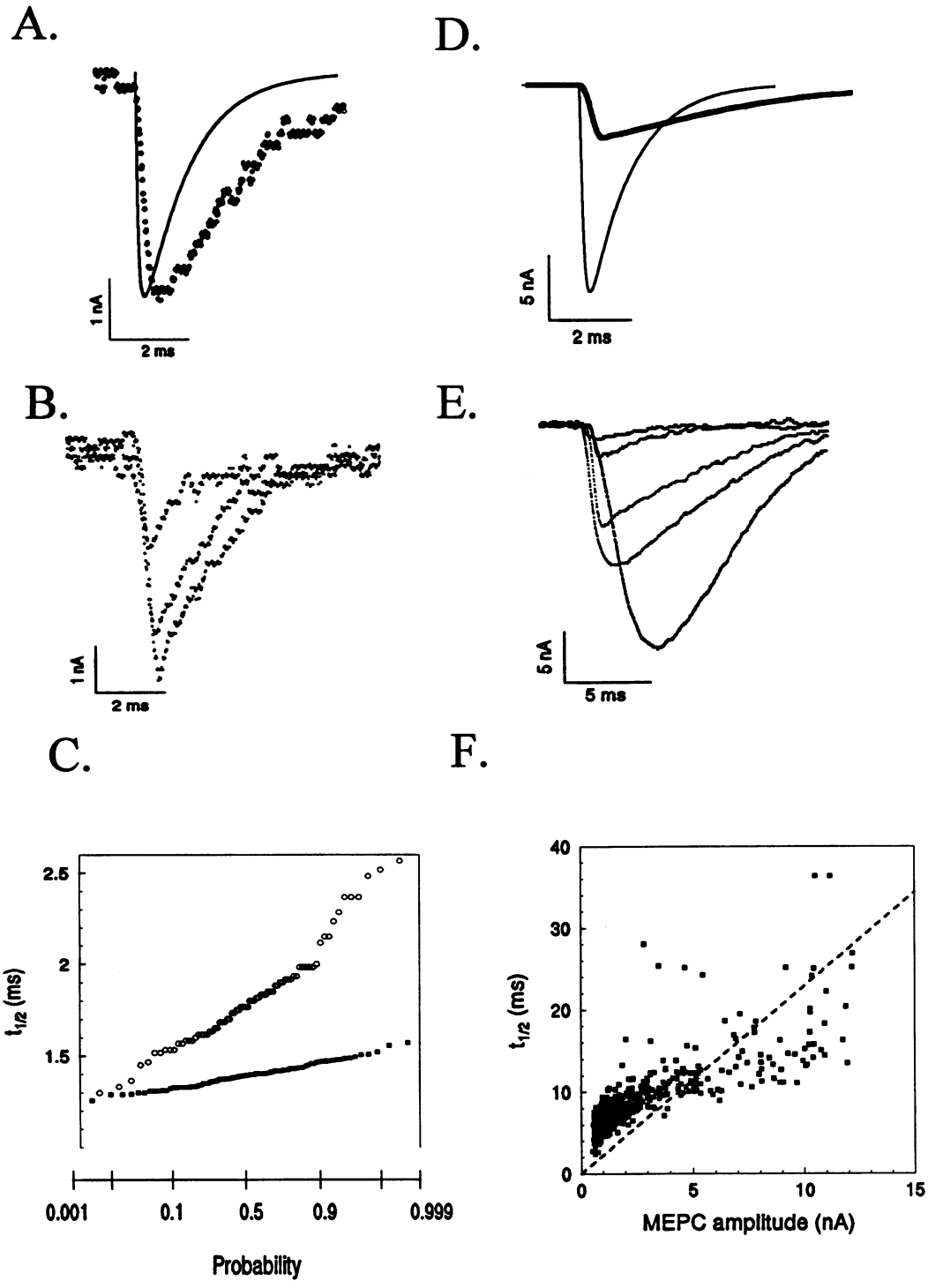

FIGURE 2 Properties of MEPCs compared to model MEPCs. (*A*) ·····, An MEPC recorded from an untreated frog sartorius muscle clamped at −80 mV at 22.3°C. This MEPC was one of the longest in the data set. ——, A modeled MEPC. (*B*) Some of the variety of MEPCs recorded in the same set. (*C*) Plots of actual and modeled half decay times on a probability abscissa. Data fitting a normal probability distribution function falls along a straight line when plotted on a probability abscissa. The plot shows that the half decay times of MEPCs are not normally distributed. The sizes of the MEPCs also do not fit well to a normal distribution (Van der Kloot, 1991b). ○, The half-times of MEPC decays from the data set. ■, The distribution of half-times predicted by a model in which the decay is determined solely by the open time of endplate channels. (*D*) *Dense line*, Averaged MEPCs from a preparation pretreated with 1 μM PGE_2, −80 mV, 20.2°C. *Light line*, A calculated MEPC, in which the number of AChs released was increased so that roughly the same number of channels were opened by the MEPC and the model, i.e., their areas are equal. (*E*) MEPCs from a set recorded from a sartorius muscle soaked for 2 h in Ringer's in which the NaCl was replaced with 200 mM Na gluconate. The recording was done in Ringer's at −80 mV at 22.3°C. This was the contralateral muscle from that used for the recordings shown in Fig. 1 *A*. (*F*) A plot of the $t_{1/2}$s of 198 MEPCs from a junction in a muscle pretreated in gluconate solution as a function of their amplitudes. The recording was done at −100 mV at 22.3°C. For the regression line $R^2 = 0.92$. The fitting of the regression line was constrained to run through 0, 0.

(Edmonds et al., 1995). Therefore it is unlikely the scatter is caused solely by postsynaptic diversity.

Other evidence in the literature supports the conclusion that MEPC decay in normal preparations can be slower than predicted from channel closings. The mean open time for the endplate channels is obtained from measurements of the endplate current fluctuations recorded during the sustained application of ACh (Anderson and Stevens, 1973). Since the fluctuation method was developed it has been found that often the open period of the endplate channels is interrupted by very brief closings. Such closings will not substantially alter the power spectra of the ACh fluctuations (Edmonds et al., 1995). The decay of averaged MEPCs is slower than predicted by the measurements of channel mean opening time in toad, frog, and human muscle (Colquhoun et al., 1977; Gage and Van Helden, 1979; Katz and Miledi, 1973; Cull-Candy et al., 1979). Previously we recorded MEPCs and then used the fluctuation method to determine the mean channel conductances and open times on the same fibers (Van der Kloot et al., 1994). Then we employed a deconvolution method to calculate when individual channels would have to open to generate individual or averaged MEPCs (Cohen et al., 1981). Frequently the results showed that the initial surge of channel opening was followed by a tail of continued opening. This tail accounts for the lengthening of the MEPC decay.

Decay times of large quanta

There is an even greater discrepancy between the classical model and MEPCs recorded from preparations treated to increase quantal size. Size can be increased by activating protein kinase A, either with permeable cAMP derivatives or epinephrine, or by soaking in hypertonic solutions (Van der Kloot and Van der Kloot, 1986; Van der Kloot, 1987, 1991b; Van der Kloot and Branisteanu, 1992). Size can also be increased by insulin or by PGE_2, working by intracellular signaling pathways yet to be identified. Size increases because more ACh is released per quantum. As shown in Fig. 2 *D* the discrepancy between the classical model and the decay of MEPCs is even more striking when the quanta contain more ACh. In this example the model was scaled so that it opened the same number of channels as the MEPC. Fig. 2 *E* shows examples of the variations in MEPC shape seen after quantal size was increased by soaking in hypertonic Na gluconate solution. For reasons we do not yet understand, this treatment produces the largest increases in size; the mean increase is almost fourfold (Van der Kloot, 1987). These exceptionally large MEPCs illustrate forcefully the problems faced by the classical model. In the classical model, when more ACh is released, the MEPC amplitude increases, the rise time is lengthened, but decay is still determined by the mean channel open time. In reality there is significant correlation between MEPC amplitudes and decay times: the larger the amplitude, the slower the decay (Fig. 2 *F*). This correlation was observed in scores of examples, regardless of whether the regression line was constrained to pass through 0,0. Deconvolutions of the enlarged MEPCs show that channels continue to open for 10 ms or even longer (see Van der Kloot, 1991b, figure 20).

Modifying the model to account for the relation between amplitude and decay time

The correlation of amplitude and decay time is not predicted by either the classical or the pore model (Fig. 3 *A* shows the classical model). Release through a pore will slow MEPC rise and decay times. However, it does not predict that the decay time will lengthen when the concentration of ACh in

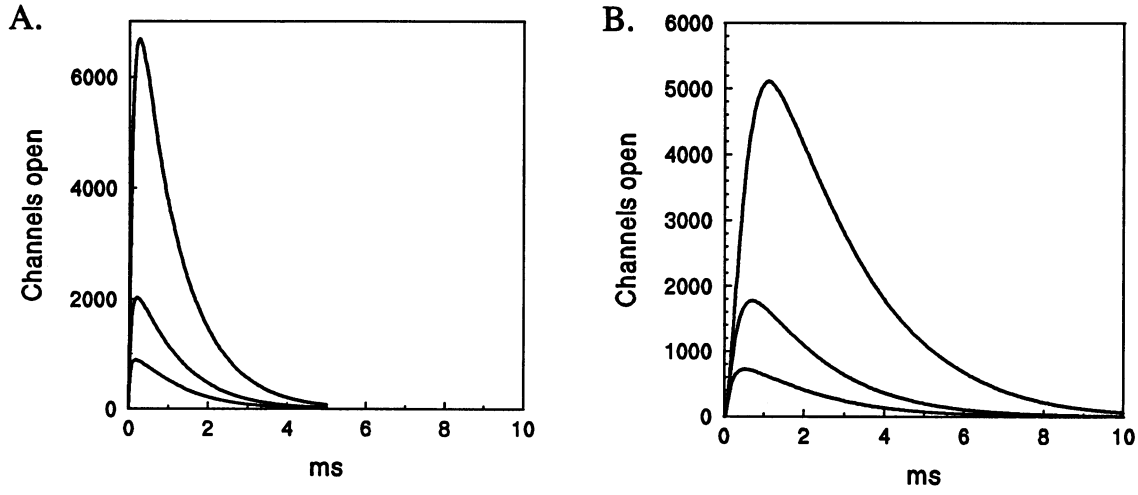

FIGURE 3 Model MEPCs calculated by the classical model of Wathey et al. (1979) with different quantities of ACh in the quanta. (*A*) The model in which all of the ACh is released at time 0. (*B*) The ACh is released from a vesicle through a pore according to Eq. 1. Values used: $r_o = 0.08 \times 10^{-6}$ cm; $L = 1 \times 10^{-6}$ cm; $D = 4 \times 10^{-6}$ cm^2 s^{-1}. When the quantum contained 10,000 ACh molecules the vesicle volume was 2.65×10^{-17} cm^3. As the ACh content was varied, the vesicle volume was changed to keep the ACh concentration in the vesicle constant.

the vesicle is increased. The amount released from the vesicle, c_r, in time t is described by

$$C_r = C_o\left\{1 - \exp\left(\frac{-t}{VL/(\pi r_o^2 D)}\right)\right\}, \quad (8)$$

where C_o is the amount initially in the vesicle, V is the vesicular volume, L is the length of the pore, r_o is the radius of the pore, and D is the diffusion coefficient for the ACh in the pore (Almers et al., 1991). The efflux is proportional to C_o, but an increase in C_o does not extend the period of release.

Suppose, however, that the vesicles enlarge as they are loaded further, so their concentration of ACh does not increase but their volume (V in Eq. 8) increases. When a pore opens between the vesicle interior and the synaptic cleft, the duration of ACh efflux depends upon the volume of the vesicle: the larger the vesicle, the longer the period of efflux and the slower the decay of the MEPC (Fig. 3 *B*). If the vesicles enlarge as they acquire additional ACh, this would also solve the problem of how the amount of ACh required to produce the largest MEPCs could possibly be packed into a vesicle of the size seen in the cytoplasm (Van der Kloot, 1991b). The expanding vesicle model accounts nicely for the properties of the MEPC.

Second-stage loading

The usual picture is that the vesicles are formed and receive their quota of ACh in the cytoplasm. They then are fastened at an active zone before they can be released. Doherty et al. (1984, 1986) showed that this picture is incomplete. They found that transitorily increasing the rate of quantal release led to a transitory fall in MEPP amplitude. Their interpretation is that the quanta receive part of their complement of ACh while they are fastened at the active zones. During stimulation quanta are released before they have time to acquire their usual increment of ACh. In untreated preparations about 17% of the ACh is added to the stockpile of quanta awaiting release. They estimated the size of this stockpile at about 10,000, roughly the number of vesicles positioned at the active zones. We have named the process that adds more ACh to vesicles on the active zone second-stage loading (Yu and Van der Kloot, 1991; Van der Kloot, 1991b).

An additional role for second-stage loading became apparent when we discovered that after the ACh content of the quanta had been experimentally increased, the process could be reverted, so the quanta returned to normal size. This could be done by activating protein kinase C, or by exposing the preparation to micromolar concentrations of nicotinic agonists (Van der Kloot, 1991a, 1993). These treatments appear to turn off the production of additional large quanta, but leave the terminal with a pre-existing store of the large quanta. These must be released before all quanta again are of normal size. We estimated the size of this pre-existing store at 10,000–20,000 large quanta.

Further evidence for the role of second-stage loading came from studies of the effects of inhibitors of active ACh transport into isolated synaptic vesicles, like (−)-vesamicol (Anderson et al., 1983; Prior et al., 1992). We found that exposure to these inhibitors reduced the sizes of large MEPCs and of MEPCs recorded when AChE was inhibited (Yu and Van der Kloot, 1991; Van der Kloot et al., 1994; Naves and Van der Kloot, manuscript in preparation). These MEPCs can also be made smaller by treatment with hemicholinium-3 (HC-3), which blocks choline uptake into nerve terminals (Fig. 4 *A*). The changes are just like those produced by 2 μM (−)-vesamicol (n = 6). Our interpretation is that lowering the cytoplasmic concentration of ACh decreases second-stage loading, and therefore the quanta become smaller (Fig. 4 *B*).

Second-stage loading can be followed by altering the transmitter loaded into the vesicles. The false transmitter acetylmonoethylcholine (AMECH), on average, opens endplate channels for only about half the duration they are opened by ACh (Colquhoun et al., 1977; Large and Rang, 1978). Therefore, when a quantum contains AMECH the MEPC decays roughly twice as fast as normally. The AMECH is also less efficacious in opening endplate channels, so the amplitude of the MEPC is reduced. The nerve terminals synthesize AMECH when the extracellular solution contains monoethylcholine (MECH). The MECH is brought into the nerve terminal and acetylated to AMECH, which is then stored in the synaptic vesicles.

In the following experiments all of the solutions contained 10 μM neostigmine to minimize recycling of precursor (Van der Kloot et al., 1995). Preparations were kept for 2 h in 200 mM Na gluconate solution containing 0.4 mM MECH. They were then transferred to Ringer's, and a junction was voltage clamped at a holding potential close to that observed after both electrodes were inserted. Then the solution was changed to Ringer's containing 10 μM choline

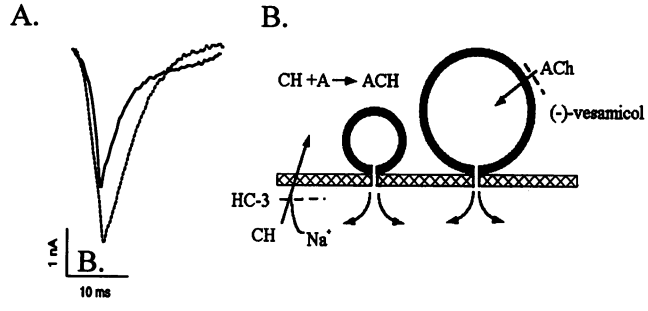

FIGURE 4 (*A*) Averaged MEPCs from a muscle pretreated in hypertonic gluconate solution and the effects of HC-3. Recorded in Ringer's at −90 mV and 15°C. *Larger MEPC*, Average of 39 recorded in Ringer's. *Smaller MEPC*, 103 recorded from the same junction after 48 min in 2 μM HC-3. The HC-3 reduced the amplitude to 77% and the decay time to 80%. Similar results were obtained in five additional experiments. (*B*) Diagram of the proposed mechanism. Vesicles preloaded with ACh in the cytoplasm attach at the active zones. While there they receive additional increments of ACh. Release occurs through a pore between the vesicle interior and the synaptic cleft.

(CH). Both ∫MEPCs and the times at which they were measured were recorded for many minutes. Fig. 5 *A* summarizes one of these experiments. The bins are averages of 20 sequentially recorded ∫MEPCs. The ∫MEPCs had a substantial variance, so that there was also considerable variation in the averages. Nonetheless, there was a clear upward trend in the averages. This suggests that MEPC size was increasing. The distributions of ∫MEPCs in the first 100 recorded and the last 100 recorded, shown in the insert, establish that there was a significant increase in quantal size during the period of observation. We can roughly estimate the number of quanta released during the period of observation. About 1100 MEPCs were recorded. By observing the oscilloscope screen during the experiment we estimated that at the very least we measured one-fifth of the MEPCs released, so our estimate of the maximum number of quanta released as the quantal size was almost doubled is 5500. This contrasts with the estimate of about 300,000 vesicles per junction, of which about 20,000 are positioned at the active zones (Van der Kloot and Molgó, 1994). These results were replicated twice more.

Similar experiments were done to follow the incorporation of AMECH into the quanta. After 2 h in 200 mM sodium gluconate solution, the preparations were placed in Ringer's and a junction was voltage clamped. Then the solution was changed to Ringer's containing 0.4 mM MECH and the MEPCs were recorded for a least 40 min. Fig. 5 *B* shows that during the period of observation the ∫MEPCs decreased in size. The insert shows that the first 100 and last 100 MEPCs recorded are significantly different. Again the change occurred as the terminal released 5000 or fewer vesicles (the observations were replicated in two additional experiments).

Our picture is that a large number of vesicles containing ACh are clustered in the cytoplasm. When positions at the active zones become vacant, vesicles from the cytoplasm attach. Once attached they acquire more ACh by second-stage loading (Fig. 4 *B*). Usually second-stage loading increases the ACh content by about 17%. After treatments that increase quantal size, the ACh content can be increased by 100–300% (Van der Kloot, 1987, 1991b).

A model to account for the skew in quantal size distributions

Second-stage loading seemed to offer a possible explanation for the skewed distribution of quantal sizes. To test this idea, we developed a Monte Carlo model that includes second-stage loading. The vesicles are formed in the cytoplasm; the quantities of ACh they contain are normally distributed. The vesicles then attach to release sites. While on the active zone they continually acquire more ACh. Release is random; there is no increase in the probability of release when the vesicles contain more ACh. Three examples of the predictions of this model are shown in Fig. 6 *A*. The distribution of MEPC sizes is no longer gaussian, as shown by the upward curves in the plots of the data on a probability axis. Like actual MEPC distributions, plots of the logarithms of the sizes of the modeled quanta fall much closer to normal probability distributions (Fig. 6 *B*).

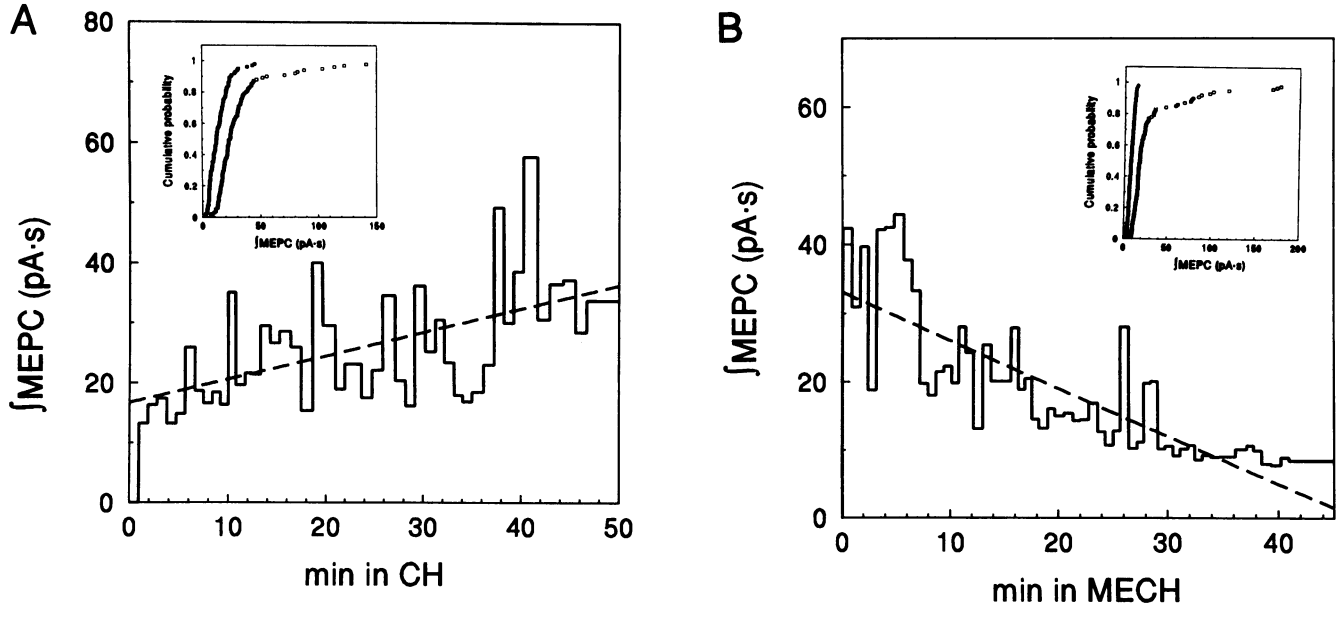

FIGURE 5 Experiments on the incorporation of different transmitters into quanta released from gluconate-treated muscles. All solutions contained 10 μM neostigmine. (*A*) Muscle pretreated for 2 h in 200 mM gluconate + 0.4 mM MECH. In Ringer's, junction clamped at −88 mV. At time 0 10 μM CH was added to the solution. (*B*) Muscle pretreated for 2 h in 200 mM gluconate. Ringer's, junction clamped at −90 mV. At time 0 400 μM MECH was added to the solution. Further explanation in text.

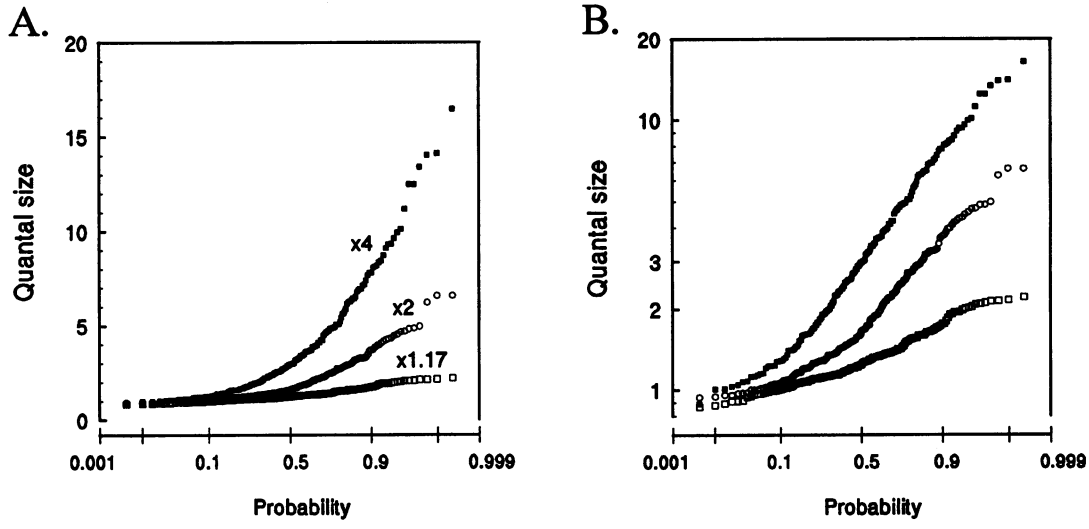

FIGURE 6 The distribution of quantal sizes predicted by a model in which the vesicles are first loaded with ACh in the cytoplasm, and then, after they are attached at active zones, continue to acquire ACh at a steady rate until they are released by chance. Three rates of second-stage loading were modeled, which brought the final ACh content to different proportions of the initial vesicle content. □, To 117%; ○, to 200%; ■, to 400%. (*A*) On a probability plot. (*B*) The logarithms of the modeled sets are plotted to show that the distributions are more linear, as is the case with real data.

DISCUSSION AND CONCLUSIONS

The classical picture of ACh release at the neuromuscular junction, in which the entire quantal content is dumped instantaneously into the synaptic cleft, predicts rise times faster than those observed at the frog neuromuscular junction. One possibility is that the rise times are not accurately recorded. When an external electrode is used, the rise times might be prolonged by the "compression artifact" (Katz and Miledi, 1973). The artifact appears to be caused by the external electrode pressing down on the nerve, which narrows the synaptic cleft, thereby restricting ACh diffusion. In the frog the artifact is small in normal circumstances, at most about a 23% increase (Katz and Miledi, 1973). When acetylcholinesterase is inhibited, compression can almost double the rise time. We tried to avoid compression by using electrodes with fine tips and by backing away the electrode from the preparation once external MEPPs were detected. In the frog the rise times measured with extracellular electrode without obvious compression and with the two-electrode voltage clamp are comparable (the literature is summarized by Van der Kloot, 1995).

Stiles et al. (1995) explored the compression artifact at the lizard neuromuscular junction, where the rise time is less than 100 μs. They showed that compression with an extracellular electrode could double the rise time of MEPCs measured with the two-electrode voltage clamp, even though acetylcholinesterase was not inhibited. This shows clearly that caution is required in interpreting the measurements with external electrodes. This is especially true because the external electrodes record an unexpectedly large proportion of the MEPPs at junction (references in Van der Kloot, 1996), which suggests that we really do not understand the equivalent circuit for extracellular recording. We think the weight of evidence at the frog neuromuscular junction suggests that the rise times are slower than predicted by the classical model. The discrepancy is especially striking for the most slowly rising miniatures in each data set.

After quantal size has been increased, the decay times of many of the MEPCs are also strikingly longer than predicted by the model. To produce such long MEPCs, endplate channels must continue to open for as long as 10 ms after the beginning of the signal (Van der Kloot, 1991b, figure 20). In untreated preparations, there are almost always some MEPCs that are notably long. The present results show that in untreated preparations the variance of the decay times is substantially greater than that predicted by the model.

One way to account for the slower than predicted rise times and the longer than predicted durations is by modifying the model so that the ACh is released through a pore extending from the interior of the synaptic vesicle to the synaptic cleft. However, even with this modification the model does not predict the observed correlation between MEPC amplitude and decay time. If we modify the model by assuming that as more ACh is added the volume of the vesicles increases, then the predictions of the model are much more like real MEPCs. An increase in vesicle size would also solve the problem of how the quantity of ACh released in the largest quanta could be packed into a vesicle of usual size (Van der Kloot, 1991b) and would not require the ACh transporter to work against an increasing gradient of ACh across the vesicular membrane.

However, the sizes of the vesicles in the nerve terminal before and after treatments that increase quantal size are indistinguishable (Spielholz and Van der Kloot, 1987). This

does not disprove the hypothesis, because there is substantial evidence that some of the ACh is added to the quanta by second-stage loading, presumably when the vesicles are at the active zones (Doherty et al., 1984, 1986; Yu and Van der Kloot, 1991; Van der Kloot, 1993). The results with MECH clearly show how important second-stage loading is after quantal size has been increased. Therefore our hypothesis is that when quantal size has been enlarged, some of the vesicles at the active zone should be appreciably larger than those in the cytoplasm. This hypothesis can be tested.

Second-stage loading can also account nicely for the skew to the right seen in distributions of quantal sizes and decay times. It also accounts for the numerous observations showing that newly synthesized ACh is released preferentially (references in Tauc, 1982). Our model of second-stage loading suggests that this process accounts for the skew that is commonly observed in the distribution of miniature amplitudes, sizes, and decay times. This model can be tested further by experiments in which nerve stimulation is used to rapidly release many of the quanta at the active zones.

The evidence presented in this paper for second-stage loading and the correlation between amplitude and decay time comes largely from preparations in which quantal size has been increased. However, similar results are obtained from untreated junctions when the AChE is inhibited (Naves and Van der Kloot, manuscript in preparation). (The inhibition of the AChE probably allows the tail of ACh release to open channels rather than be destroyed before reaching the endplate; see Van der Kloot et al., 1994, figure 11.)

Obviously at present we have little idea of how applicable these ideas are to transmission at central synapses. They are attractive because it seems that the hypothesis that quantal responses at central synapses have almost no variance appears to be incorrect (Walmsey, 1995), and because the size of the quantal responses is skewed to the right, as they are for MEPCs (Bekkers et al., 1991; reviewed by Edwards, 1995). The skew is also apparent at crayfish and *Drosophilia* neuromuscular junctions (Cooper et al., 1995).

To summarize, we suggest that a number of features of MEPCs can be accounted for by modifying the classical model, supposing that release is through a pore from a vesicle whose size varies with its ACh content. Other explanations for the observed features of the MEPCs are surely possible. The present hypothesis can be tested experimentally by measuring vesicle sizes at the active zones. Release by way of a pore also may help to account for the substantial body of data suggesting that at the neuromuscular junction in some conditions the membrane of the vesicle ultimately fuses into the terminal membrane, whereas in other instances the vesicle releases its contents and returns directly to the cytoplasm (Colasante and Pécot-Dechavassine, 1995; reviewed by Van der Kloot and Molgó, 1994). In some circumstances the pore may open and then close, so that the empty vesicle is restored to the cytoplasm. In other circumstances the pore may open and continue to expand until the vesicle membrane is fused to the terminal membrane. If these two modes of release exist, it is conceivable that the rise times of MEPCs will vary according to the mode employed.

We are grateful to Drs. G. J. Baldo, R. Cameron, and I. S. Cohen for critical readings of drafts of the manuscript.

Supported by U.S. Public Health Service award NS 10320. LAN was a scholar of the Brazilian Conselho Nacional de Pesquisa (CNPq).

REFERENCES

Almers, W., L. J. Breckenridge, A. Iwata, A. K. Lee, A. E. Spruce, and F. W. Tse. 1991. Millisecond studies of single membrane fusion events. *Ann. N.Y. Acad. Sci.* 636:318–327.

Anderson, C. R., and C. F. Stevens. 1973. Voltage clamp analysis of acetylcholine produced end-plate current fluctuations at frog neuromuscular junction. *J. Physiol. (Lond.).* 235:655–691.

Anderson, D. C., S. C. King, and S. M. Parsons. 1983. Inhibition of [3H]acetylcholine active transport by tetraphenylborate and other anions. *Mol. Pharmacol.* 24:55–9.

Anglister, L., J. R. Stiles, and M. M. Salpeter. 1994. Acetylcholinesterase density and turnover number at frog neuromuscular junctions, with modeling of their role in synaptic function. *Neuron.* 12:783–794.

Bartol, T. M., B. R. Land, E. E. Salpeter, and M. M. Salpeter, M. M. 1991. Monte Carlo simulation of miniature endplate current generation in the vertebrate neuromuscular junction. *Biophys. J.* 59:1290–1307.

Bekkers, J. M., G. B. Richardson, and C. F. Stevens. 1991. Origin of variabilty in quantal size in cultured hippocampal neurons and hippocampal slices. *Proc. Natl. Acad. Sci. USA.* 87:5359–5362.

Chow, R. H., L. Von Ruden, and E. Neher. 1992. Delay in vesicle fusion revealed by electrochemical monitoring of single secretory events in adrenal chromaffin cells. *Nature.* 356:60–63.

Cohen, I., W. Van der Kloot, and D. Attwell. 1981. The timing of channel opening during miniature end-plate currents. *Brain Res.* 223:185–189.

Colasante, C., and M. Pecot-Dechavassine. 1995. Cd^{2+} and K^{+}-evoked ACh release induce different synaptophysin and synaptobrevin immunolabelling at the frog neuromuscular junction. *J. Neurocytol.* 24: 547–558.

Colquhoun, D., W. A. Large, and H. P. Rang. 1977. An analysis of the action of a false transmitter at the neuromuscular junction. *J. Physiol. (Lond.).* 266:361–395.

Cooper, R. L., B. A. Stewart, J. M. Wojtowicz, S. Wang, and H. L. Atwood. 1995. Quantal measurements and analysis methods compared for crayfish and Drosophila neuromuscular junctions, and rat hippocampus. *J. Neurosci. Methods.* 61:67–78.

Cull-Candy, S. G., R. Miledi, and A. Trautmann. 1979. End-plate currents and acetylcholine noise at normal and myasthenic human end-plates. *J. Physiol. (Lond.).* 287:247–265.

Doherty, P., B. J. Hawgood, and I. C. H. Smith. 1984. Changes in miniature end-plate potentials after brief nervous stimulation at the frog neuromuscular junction. *J. Physiol. (Lond.).* 356:349–358.

Doherty, P., B. J. Hawgood, and I. C. H. Smith. 1986. Changes in miniature end-plate potentials due to moderate hypertonicity at the frog neuromuscular junction. *J. Physiol. (Lond.).* 376:1–11.

Dwyer, T. M. 1981. The rising phase of the miniature endplate current at the frog neuromuscular junction. *Biochim. Biophys. Acta.* 646:51–60.

Edmonds, B., A. J. Gibb, and D. Colquhoun. 1995. Mechanisms of activation of muscle nicotinic acetylcholine receptors and the time course of endplate currents. *Annu. Rev. Physiol.* 57:469–493.

Edwards, F. A. 1995. Patch-clamping in brain slices: synaptic transmission from ATP to long-term potentiation. *J. Neurosci. Methods.* 59:59–65.

Faber, D. S., W. S. Young, P. Legendre, and H. Korn. 1992. Intrinsic quantal variability due to stochastic properties of receptor-transmitter interactions. *Science.* 258:1494–1498.

Gage, P.W., and D. Van Helden. 1979. Effects of permeant monovalent cations on end-plate channels. *J. Physiol. (Lond.).* 288:509–528.

Katz, B. 1969. The Release of Neural Transmitter Substances. Liverpool University Press, Liverpool. 1–60.

Katz, B., and R. Miledi. 1973. The binding of acetylcholine to receptors and its removal from the synaptic cleft. *J. Physiol. (Lond.).* 231: 549–574.

Large, W. A., and H. P. Rang. 1978. Factors affecting the rate of incorporation of a false transmitter into mammalian motor nerve terminals. *J. Physiol. (Lond.).* 285:1–24.

Madsen, B. W., R. O. Edeson, H. S. Lam, and R. K. Milne. 1984. Numerical simulation of miniature endplate currents. *Neurosci. Lett.* 48:67–74.

Magleby, K. L., and C. F. Stevens. 1972. A quantitative description of end-plate currents. *J. Physiol. (Lond.).* 223:173–197.

Monck, J. R., and J. M. Fernandez. 1992. The exocytotic fusion pore. *J. Cell Biol.* 119:1395–1404.

Nanavati, C., and J. M. Fernandez. 1993. The secretory granule matrix: a fast-acting smart polymer. *Science.* 259:963–965.

Nigmatullin, N. R., V. A. Snetkov, E. E. Nikol'skii, and L. G. Magazanik. 1988. Modelling of miniature endplate current. *Neirofiziologiia.* 20: 390–397.

Parnas, H., M. Flashner, and M. E. Spira. 1989. Sequential model to describe the nicotinic synaptic current. *Biophys. J.* 55:875–884.

Prior, C., I. G. Marshall, and S. M. Parsons. 1992. The pharmacology of vesamicol—an inhibitor of the vesicular acetylcholine transporter. *Gen. Pharmacol.* 23:1017–1022.

Rosenberry, T. L. 1979. Quantitative simulation of endplate currents at neuromuscular junctions based on the reaction of acetylcholine with acetycholine receptor and acetylcholinesterase. *Biophys. J.* 26:263–290.

Salpeter, M. M. 1987. Vertebrate neuromuscular junctions: general morphology, molecular organization, and functional consequences. *In* The Vertebrate Neuromuscular Junction. M. M. Salpeter, editor. Alan R. Liss, New York. 1–54.

Sokal, R. R., and F. J. Rohlf. 1981. Biometry. W. H. Freeman, New York. 1–859.

Spielholz, N., and W. Van der Kloot. 1987. Quantal size increases without detectable change in vesicle size at the frog neuromuscular junction. *J. Physiol. (Lond.).* 382:157P.

Spruce, A. E., L. J. Breckenridge, A. K. Lee, and W. Almers. 1990. Properties of the fusion pore that forms during exocytosis of a mast cell secretory vesicle. *Neuron.* 4:643–654.

Stavitzky, A., and J. Golay. 1964. Smoothing and differentiation of data by simplified least square procedure. *Anal. Chem.* 36:1627–1639.

Stiles, J. R., D. Van Helden, and M. M. Salpeter. 1995. Simultaneous intra- and extracellular recordings of miniature endplate currents reveal a median rise time less than 100 μs. *Soc. Neurosci. Abstr.* 21:587.

Tauc, L. 1982. Nonvesicular release of neurotransmitter. *Physiol. Rev.* 62:857–892.

Van der Kloot, W. 1987. Pretreatment with hypertonic solutions increases quantal size at the the frog neuromuscular junction. *J. Neurophysiol.* 57:1536–1554.

Van der Kloot, W. 1989. Statistical and graphical methods for testing the hypothesis that quanta are made up of subunits. *J. Neurosci. Methods.* 27:81–89.

Van der Kloot, W. 1991a. Down-regulation of quantal size at frog neuromuscular junctions: possible roles for elevated intracellular calcium and for protein kinase C. *J. Neurobiol.* 22:204–14.

Van der Kloot, W. 1991b. The regulation of quantal size. *Prog. Neurobiol.* 36:93–130.

Van der Kloot, W. 1993. Nicotinic agonists antagonize quantal size increases and evoked release at frog neuromuscular junction. *J. Physiol. (Lond.).* 468:567–589.

Van der Kloot, W. 1995. The rise times of miniature endplate currents suggest that acetylcholine may be released over a period of time. *Biophys. J.* 69:148–154.

Van der Kloot, W. 1996. Spontaneous and uniquantal evoked endplate currents in normal frogs are indistinguishable. *J. Physiol. (Lond.).* 492: 155–162.

Van der Kloot, W., O. P. Balezina, J. Molgo, and L. A. Naves. 1994. The timing of channel opening during miniature endplate currents at the frog and mouse neuromuscular junctions: effects of fasciculin-2, other anticholinesterases and vesamicol. *Pflugers Arch. Eur. J. Physiol.* 428: 114–126.

Van der Kloot, W., and D. D. Branisteanu. 1992. Effects of activators and inhibitors of protein kinase A on increases in quantal size at the frog neuromuscular junction. *Pflugers Arch. Eur. J. Physiol.* 420:336–341.

Van der Kloot, W., and J. Molgó. 1994. Quantal acetylcholine release at the vertebrate neuromuscular junction. *Physiol. Rev.* 74:899–992.

Van der Kloot, W., L. A. Naves, and O. P. Balezina. 1995. Using monoethylcholine as a false transmitter precursor to study quantal turnover at the neuromuscular junction. *Fourth IBRO World Congress of Neuroscience Abstracts.* 173.

Van der Kloot, W., and T. E. Van der Kloot. 1986. Catecholamines, insulin and ACTH increase quantal size at the frog neuromuscular junction. *Brain Res.* 376:378–81.

Walmsley, B. 1995. Interpretation of "quantal" peaks in distributions of evoked synaptic transmission at central synapses. *Proc. R. Soc. Lond.* 261:245–250.

Wathey, J. C., M. M. Nass, and H. A. Lester. 1979. Numerical reconstruction of the quantal event at nicotinic synapses. *Biophys. J.* 2:145–164.

Yu, S.P., and W. Van der Kloot. 1991. Increasing quantal size at the mouse neuromuscular junction and the role of choline. *J. Physiol. (Lond.).* 433:677–704.